Available online at www.sciencedirect.com
SCIENCE DIRECT
Scripta Materialia 54 (2006) 1059–1063
Scripta MATERIALIA
www.actamat-journals.com

Grain boundary energy and grain growth in Al films: Comparison of experiments and simulations

K. Barmak [a,*], J. Kim [a], C.-S. Kim [a], W.E. Archibald [a], G.S. Rohrer [a], A.D. Rollett [a], D. Kinderlehrer [b], S. Ta'asan [b], H. Zhang [c], D.J. Srolovitz [c]

[a] Department of Materials Science and Engineering, Carnegie Mellon University, Pittsburgh, PA 15213, United States
[b] Department of Mathematical Sciences, Carnegie Mellon University, Pittsburgh, PA 15213, United States
[c] Princeton Institute for the Science and Technology of Materials, Department of Mechanical and Aerospace Engineering, Princeton University, Princeton, NJ 08540-5211, United States

Received 18 May 2005; received in revised form 25 July 2005; accepted 21 November 2005
Available online 22 December 2005

Abstract

Relative free energies of ⟨1 1 1⟩ tilt boundaries in 1.7-μm-thick Al films were compared with boundary enthalpies obtained via molecular dynamics simulations. Grain growth studies in 25 and 100-nm-thick Al films were compared with simulations. The sources of the differences between experimental and simulational results are discussed.

Keywords: Grain boundary energy; Grain growth; Al; Thin films; Tilt boundaries

1. Introduction

To engineer the grain boundary network and to tailor the grain structure of materials, it is of interest to develop predictive models of grain growth that incorporate experimentally determined boundary properties. To achieve this, comparison of experimentally measured boundary properties and grain structure statistics with those obtained from simulations are an obvious and necessary step. The aim of this paper is to make such comparisons for Al (films). The paper begins with a brief description of the experimental and simulational procedures before comparing the experimental and simulational results on grain boundary energy and grain growth.

2. Experimental and simulational procedures

The Al films prepared for grain boundary energy measurements were 1.7 μm-thick and were sputter deposited onto oxidized silicon wafers and annealed at 450 °C (723 K) for 5 h in Ar–4%H_2. The silicon dioxide thickness was 100 nm. The Al sputtering target was 99.99% pure. The total metallic impurity content of the target was 5.6 ppm by atom, with Fe accounting for 3.0 ppm of this total. The Si content was 1.8 ppm. The total amount of non-metallic impurities with significant concentrations, namely H, C, N, O, and P was 17.5 ppm. The strong ⟨1 1 1⟩ fiber texture of the Al film following annealing allied with a nearly columnar grain structure meant that almost all of the boundaries had tilt character and a common ⟨1 1 1⟩ axis.

Crystal orientation maps on planar sections of the film were obtained using an electron backscatter diffraction (EBSD) mapping system (TexSEM Laboratories, Inc.) integrated with a scanning electron microscope (Phillips XL40 FEG). Orientations were recorded at intervals of 150 nm on a hexagonal grid. The mean grain size of the film was 2.2 μm. Line segments representing the grain boundary traces were extracted from the orientation maps using a procedure described by Wright and Larsen [1]. From these segments, more than 8500 triplets meeting at a single point were identified and the dihedral angles were

* Corresponding author.
E-mail address: katayun@andrew.cmu.edu (K. Barmak).

1359-6462/$ - see front matter
doi:10.1016/j.scriptamat.2005.11.060

determined. If all three grains were within 10° of the ⟨1 1 1⟩ orientation, it was assumed that all three boundaries could be considered as [1 1 1] tilt boundaries; more than 7300 of the junctions met this criterion. This simplified our analysis by allowing us to consider only a single degree of freedom: the tilt about the [1 1 1] axis. All grain boundaries were then classified according to their misorientation (equivalent to tilt) angle (with a 2° resolution), and, assuming all of the junctions to be in local equilibrium, the relative boundary energies were determined using a multi-scale reconstruction method described in an earlier paper [2]. The growth of grains during film annealing was taken to indicate that the boundaries were mobile enough for triple junctions to achieve local equilibrium. In the analysis of grain boundary energies, it was assumed that Young's equation $\gamma_i/\sin\phi_i =$ constant, where γ_i is the energy, ϕ_i is the dihedral angle, and i sums over the three boundaries at each junction describes the equilibrium at each junction. In other words, the lattice misorientation, but not the orientation of the grain boundary plane, was considered in this analysis. The error bars for the relative energies were calculated by obtaining the residual relative energy at each of the 7300 triple junctions. In principle, this residual should be zero; in practice it is not. The residual was then divided equally among the three boundaries meeting at the triple junction. The average residual for each boundary type was then calculated and reported as the error bar.

Grain growth was examined in 25 and 100-nm-thick films of Al, deposited from the same target and in the same chamber as the thicker films. Film texture for the 100-nm-thick films was characterized through pole figures. The films were found to be strongly ⟨1 1 1⟩ fiber-textured, with little strengthening of this texture upon annealing. The films were annealed in Ar–4%H_2 at 400 °C (673 K) for up to 10 h. The grain structure of the films was characterized by transmission electron microscopy. Additional details are given elsewhere [3].

The absolute values of the grain boundary enthalpy (see below) as a function of misorientation for ⟨1 1 1⟩ tilt boundaries at 154 °C (427 K) were obtained using curvature-driven grain boundary migration molecular dynamics (MD) simulations. These simulations were designed primarily to measure reduced grain boundary mobilities. The geometry of the simulation cell is shown in Fig. 1, where a U-shaped grain of one orientation is inserted into an otherwise single crystal unit cell. The width, height and thickness (d) of the simulation cell were 20, 34 and 4.2 nm, respectively. The curved section of the U-shaped grain boundary migrates towards its center of curvature such that the height of the U-shaped grain decreases with time, yet the shape of the curved section of the U remains unchanged. This geometry insures that the measured growth velocities are steady-state velocities. The absolute grain boundary enthalpy, γ, is determined from the rate of change of the (internal) energy of the system, E, in the MD simulations as the U-shaped grain retracts. Since the sides of the U-shaped grain remain nearly straight and parallel as the curved end of the loop

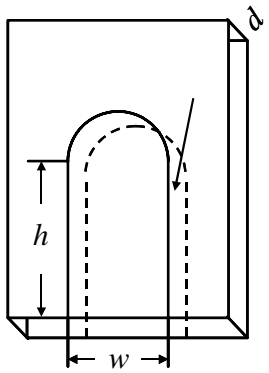

Fig. 1. The capillarity driven grain boundary migration simulation cell geometry.

migrates, the energy of the system E decreases in direct proportion to the height of the U-shaped grain h; i.e., $\Delta E = 2\gamma d\Delta h$. For a U-shaped grain of width w, this expression can be written as $\gamma = w(\mathrm{d}E/\mathrm{d}t)/2(\mathrm{d}V/\mathrm{d}t)$, where the rate of change of the grain volume is $\mathrm{d}V/\mathrm{d}t = (\mathrm{d}h/\mathrm{d}t)\mathrm{d}w$ [4]. Both $\mathrm{d}E/\mathrm{d}t$ and $\mathrm{d}V/\mathrm{d}t$ are easily measured during the simulation. This approach readily yields the grain boundary internal energy (or enthalpy), rather than the grain boundary free energy. Since the variation of the internal energy with misorientation dominates the variation of the free energy, the internal energy data provides a reasonable quantity for comparison with the experimental results (at fixed temperature). The simulations were performed using the Voter–Chen embedded atom method potential for Al [5]. Additional details are given elsewhere [4].

Grain growth simulations were performed using both the Monte Carlo Potts (MC) model and a boundary tracking model termed the partial differential equation (PDE) model [3]. The PDE simulations portray the evolution of a network of two-dimensional curves governed by the Mullins Equation of curvature driven growth [6]. The Herring Condition of force balance was imposed at each triple junction [7]. Both isotropic and anisotropic energies were used in the PDE simulations. The PDE approach resembles the grain growth simulation approach of Frost and coworkers [8]. Additional details of the simulation procedure can be found elsewhere [3].

3. Results

The relative grain boundary free energies as a function of misorientation angle are given in Fig. 2. There are deep minima at misorientation angles of 28° and 38°. Interestingly, these misorientation angles are close to those for $\sum$13 boundaries at 27.8° and $\sum$7 boundaries at 38°. As noted above, the strong ⟨1 1 1⟩ fiber texture means that the boundaries are predominantly ⟨1 1 1⟩ tilts. Therefore, the absence of a deep cusp at the $\sum$3 position is not surprising, because, in this sample, the boundaries used for the calculation were all incoherent twins. Other investigations of grain boundary energy have also found that

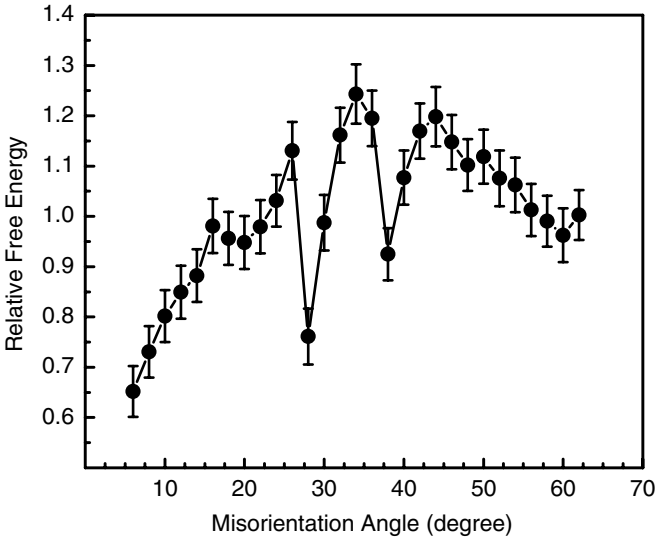

Fig. 2. Relative grain boundary free energy as a function of misorientation for a 1.7-μm-thick Al film annealed at 450 °C. The line is drawn to guide the eye.

there was no sharp cusp at the $\sum 3$ position unless coherent twin boundaries were considered [9,10].

The (rescaled) experimental relative grain boundary free energies and the grain boundary enthalpies obtained from molecular dynamics simulations are plotted together in Fig. 3 over the range of misorientation angles examined in the simulations (26–42°). Note that since the experimental energies are relative energies such rescaling is appropriate. Comparison of the experimental and simulational data sets shows that the experimental results exhibit a larger variation, i.e., a larger anisotropy, in energy than do the simulation results. The range of enthalpy values obtained from simulations is narrow (0.18–0.23 mJ/m^2). There is one exception for boundaries with a misorientation angle

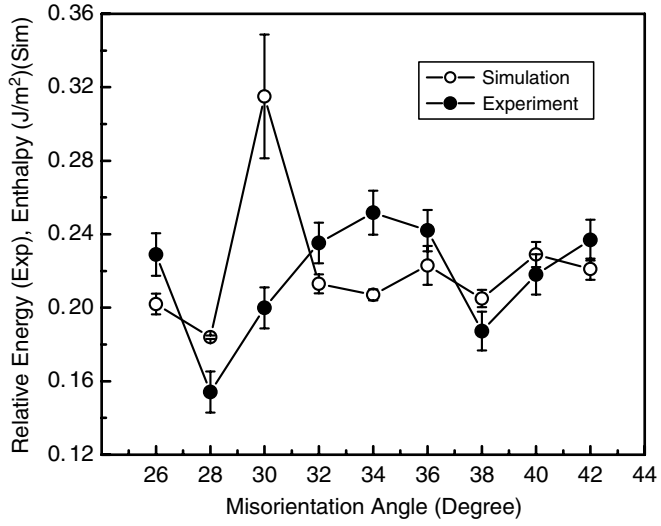

Fig. 3. Comparison of (rescaled) experimental relative grain boundary free energies and the grain boundary enthalpies obtained from molecular dynamics simulations over the range of misorientation angles examined in the simulations. The lines are drawn to guide the eye.

of 30°. The reason for the significantly higher values for this particular misorientation and the large associated error bar is not clear. Two of the minima for the simulations coincide with those for the experimental results. However, at the position of the third (shallow) minimum at 34°, the experimental results show a maximum in relative energy. The minimum in the simulation results at this angle is very shallow (less than 10 mJ/m^2) and may not be significant within the error of the simulations.

Three differences between the experiments and simulations are evident. The first is temperature. The significance of temperature lies in the fact that available evidence suggests that increased temperature decreases the anisotropy of grain boundary energy [11]. The experimental samples were annealed at 450 °C (723 K) whereas the simulations were carried out at a significantly lower temperature, namely 154 °C (427 K). The difference in temperature is diminished, if the value is normalized by the respective melting points for Al: $T/T_m = 0.77 (T_m = 933\ \mathrm{K})$ for the experiments, whereas $T/T_m = 0.70$ ($T_m = 610$ K, for the Voter–Chen potential [5]) for the simulations.

The second difference is that the experimental energies are free energies, whereas the simulations yield only the enthalpy. In general, the entropy term should decrease the grain boundary free energy relative to the enthalpy [12]. However, whether or not the entropy decreases the variation (anisotropy) of the free energy depends on the relationship between the atomic boundary structure and the energy.

The third difference between the experimental and simulational samples is the inevitable presence of impurities in the experimental sample and a complete absence of impurities in the simulated material. Impurities are usually assumed to reduce the range of energy variations. This is a common expectation, but there is little experimental data in support of this assertion. On the contrary, experiments show that impurities increase the anisotropy of surface energy, and thus potentially also that of grain boundary energies [13,14].

There is also another feasible explanation for the observed difference between experimental and simulational energies, suggested by Gottstein and Shvindlerman [11]. Several investigations have suggested that the enthalpy and entropy of migration are proportional to one another for a given series of boundaries (e.g. ⟨1 1 1⟩ tilt boundaries in Al with varying misorientation angles). The practical consequence of this observation is that a "compensation temperature" exists at which differences in mobility between boundary types are minimized. Although no such data exists for boundary energy, it is known that special boundary types exhibit transitions in structure and, therefore, energy [11,15]. It is possible that the temperature used in the simulations was close to such a compensation temperature whereas for the experiments it was not. A test for this would be to repeat both the simulations and the experiments at different temperatures and investigate the sensitivity of the anisotropy to temperature.

Table 1 gives the mean grain size, D, taken as the equivalent circular diameter, i.e., $(4A/\pi)^{1/2}$, where A is the grain area, and the standard deviation in grain size as a function of annealing time for the 100-nm-thick Al film. It is clear that grain growth stagnates after 1 h of annealing, when the grains have nearly doubled in size from 68 nm to 134 nm. The grain area distributions, given in Fig. 4, show that grain growth in the film is not self-similar, though the distributions for the different annealing times are not greatly different. The lack of self-similarity manifests itself as a slight shift of the probability distribution toward smaller reduced grain area for the stagnant structure with respect to that for 0.5 h annealed sample, and for the 0.5 h annealed sample relative to the as-deposited sample (Fig. 4). This shift to smaller area indicates an increase in the fraction of small grains with annealing. Furthermore, examination of the fraction of grains of a particular grain size (not reduced) as function of annealing given in Ref. [3] shows that the distributions are pinned at the smallest end for grains in the 1–10 nm size range. This indicates that the small grains persist in the structure longer than expected. Interestingly, at the other end of the distributions (i.e., for large grain area), the experimental grain area distributions exhibits a small (but significant) number of grains with areas that are significantly larger, 5–18 times larger, than the mean [16]. By contrast, in simulations no grains with areas more than five times the mean are seen. In other words, the experimental distributions differ from the simulated ones in that they contain more small grains and more large grains than the simulations (see also below).

Table 1
Annealing time, mean grain size, defined as the equivalent circular diameter (see text), standard deviation in grain size, and number of grains measured for 100-nm-thick Al films annealed at 400 °C

Annealing time (h)	Average grain size (nm)	Standard deviation (nm)	Number of grains measured
0 (as-deposited)	68	29	1497
0.5	87	42	1304
1	134	73	1100
2	139	68	1353
4	146	75	1455
10	137	45	2022

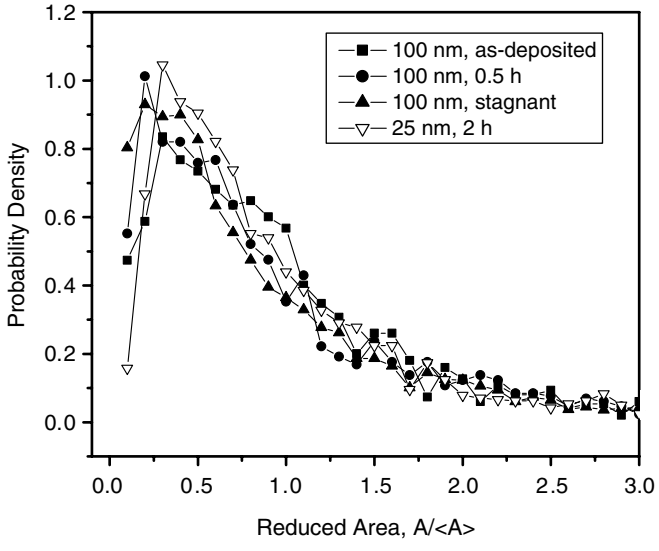

Fig. 4. Probability density for reduced grain area for 100- and 25-nm-thick Al films annealed at 400 °C. The distribution labeled as "stagnant" is the combined data for 100-nm-thick Al films annealed for 1, 2, 4 and 10 h.

Before comparing simulations and experiments for grain growth in more detail, it is useful to address the role of driving forces other than grain boundary energy reduction and the stagnation of grain growth in thin films. Driving forces other than grain boundary energy reduction that can promote grain growth in thin films include surface and elastic-strain energies [17]. The minimization of these energies favors the growth of certain subpopulation of grains and leads to the development of strong film texture [17]. However, for the films studied here, the minimization of these energies is not expected to play a significant role in either the initial grain growth or the eventual stagnation since the films were very strongly $\langle 1\,1\,1\rangle$ fiber-textured even in the as-deposited condition and annealing resulted in negligible change in this texture. In addition, the Al films are in the zero stress, or low-compressive steady-state stress state at the annealing temperature and reach this state during heating to temperature [3]. Thus, film stress and its relaxation are also not expected to play a significant role in the observed grain growth and the subsequent stagnation.

Stagnation of grain growth in thin films has been previously attributed to the pinning of grain boundaries by grooves formed at the intersection of the boundary with the film surface [18]. However, given the very stable oxide of Al formed upon exposure to air, grooves are not expected to form in this film [3,9,16]. Furthermore, grooving should pin the boundaries with low curvature, whereas Fig. 4 indicates that it is the boundaries of small grains, which by necessity have high curvature, that are the affected boundaries. A similar argument would apply to solute drag as a source of boundary pinning, since again the low curvature boundaries should be the affected boundaries [19]. More detailed analysis of the effect of solute drag shows that the level of Fe impurities in the Al films is not sufficient to pin the grain boundaries (for grains of average size), even if all the Fe were present in the grain boundaries rather than being distributed randomly throughout the film volume [16,20]. However, if all the impurities from the target ($5.6 + 1.8 + 17.5$ ppm) and potentially those introduced during sputtering and from reduction of the silicon dioxide by Al during annealing of the film were to be present at the grain boundaries, stagnation of grain growth by impurities could become feasible. Despite this point, stagnation of grain growth in the Al film cannot be attributed simply to the presence of impurities, because of the observed accumulation of small grains (with necessarily high curvature boundaries) and the presence of very large

grains (>5 times the mean area, with necessarily low curvature boundaries) in the films as they are annealed. In other words, the grain area distributions are inconsistent with solute drag as an explanation for observed stagnation of grain growth.

The MC and PDE simulations (with isotropic or anisotropic boundary energies) yield grain size distributions that were in excellent agreement with one another (not shown) [3]. There was no stagnation in growth and the distributions were found to be self-similar, as expected. Comparison of the simulated and experimental structures shows higher probabilities for small grains in the experimental samples, whether the grains are still growing (0.5 h) or whether they have reached the stagnant stage, as seen in Fig. 5. Thus, it can be concluded that grain growth in the 100-nm-thick Al films is neither well-represented by the 2D Monte Carlo model nor by the 2D PDE model. The disagreement between experiment and simulation is either a consequence of the finite thickness of the films, given that thin films are not strictly 2D systems, or it implies the need for the inclusion of other terms in the equations for grain boundary motion. The impact of the finite thickness of the films was tested by examination of a thinner film (25 nm thick). As can be seen in Fig. 3, the 25-nm- and the 100-nm-thick films show little difference in the grain size distribution. Therefore, we can rule out film thickness effects.

The question remains as to what other terms are to be included in the equations for boundary motion (or retardation) to bring simulations and experiments into agreement, given that all contributions to grain boundary drag were shown here to not apply. However, it will be useful for future simulations to use initial grain structures that are statistically equivalent to the experimental structures. At present, simulations use Voronoi structures resulting from a burst of nucleation and growth to coalescence.

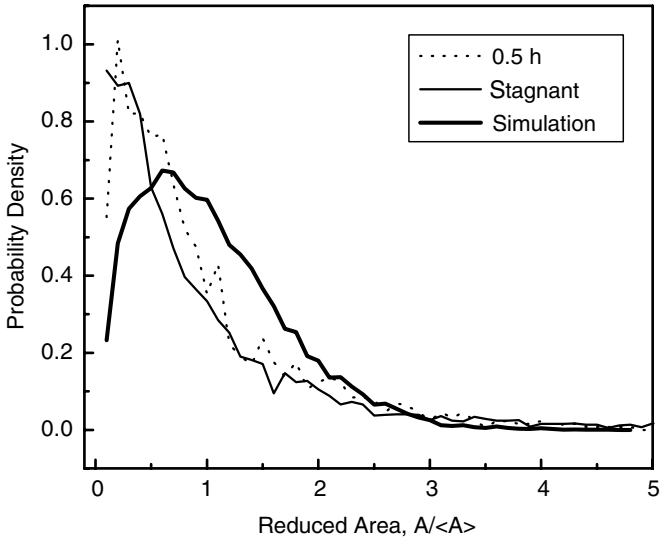

Fig. 5. Comparison of reduced grain area probability densities for simulation and experiment (100-nm-thick Al films in Fig. 4).

4. Conclusions

The variation (anisotropy) in the grain boundary energy of ⟨1 1 1⟩ tilt boundaries in a 1.7-μm-thick Al film was compared to calculated values based on molecular dynamics simulations of grain boundary migration in pure aluminum. Larger variations were found in the experimental results than in the theoretical ones. Grain growth in a 100-nm-thick Al film proceeded until the grains doubled in size, at which point it stagnated (i.e. no further growth was observed). Analysis of the range of possible solute loadings on boundaries and the form of the grain size distribution make it unlikely that solute drag accounts for the stagnation observed. However, no other physical explanation is currently apparent. Beyond the additional experiments and simulations suggested in the text, experimental studies of materials other than Al that can be obtained in purer form or are less sensitive to the presence of impurities is recommended.

Acknowledgements

Support from the MRSEC program of the NSF under DMR-0520425 is gratefully acknowledged. P. Yu and I. Livshits are thanked for their contributions.

References

[1] Wright SI, Larsen RJ. J Micros 2002;205:245.
[2] Adams BL, Kinderlehrer D, Mullins WW, Rollett AD, Ta'asan S. Scr Mater 1998;38:531.
[3] Barmak K, Archibald WE, Rollett AD, Ta'asan S, Kinderlehrer D. Mater Res Symp Proc 2004;819:N6.6-1.
[4] Zhang H, Upmanyu M, Srolovitz DJ. Acta Mater 2005;53:79.
[5] Voter AF, Chen SP. Mater Res Soc Symp Proc 1987;82:175Srinivasan SG. Private communication.
[6] Mullins WW. J Appl Phys 1956;27:900.
[7] Herring C. In: Kingston WE, editor. The physics of powder metallurgy. New York: McGraw-Hill Book Co.; 1951. p. 143.
[8] Frost HJ, Thompson CV, Howe CL, Wang J. Scr Mater 1988;22:65.
[9] Yang CC. PhD thesis, Carnegie Mellon University, Pittsburgh, 2000.
[10] Hasson GC, Goux C. Scr Metall 1971;5:889.
[11] Gottstein G, Shvindlerman LS. Grain boundary migration in metals. Boca Raton: CRC Press; 1999.
[12] Najafabadi R, Srolovitz DJ, LeSar R. J Mater Res 1991;6:999.
[13] Chatain D, Wynblatt P, Rohrer GS. Acta Mater 2005;53:4057.
[14] Hondros ED, McLean D. Philos Mag 1974;29:771.
[15] Sutton AP, Balluffi RW. Interfaces in crystalline materials. New York: Oxford University Press; 1995.
[16] Archibald WE. PhD thesis, Carnegie Mellon University, Pittsburgh, 2004.
[17] Thompson CV. Ann Rev Mater Sci 2000;30:159.
[18] Frost HJ, Thompson CV, Walton DT. Acta Metall 1990;38:1455.
[19] Frost HJ, Hayashi Y, Thompson CV, Walton DT. Mater Res Soc Symp Proc 1994;317:485.
[20] Gordon P, Bassayouni TA. Trans AIME 1965;233:391.